# Striking stability of a mixed-valence thallium(III)-thallium(I) complex in some solvents

Krzysztof Łyczko [a], Agnieszka Więckowska [b], Éva G. Bajnoczi [c,d], Tibor Csupász [e], Mihály Purgel [e], Kajsa G.V. Sigfridsson Clauss [f], Imre Tóth [e,*], Ingmar Persson [c,*]

[a] Institute of Nuclear Chemistry and Technology, Dorodna 16, PL-03-195 Warsaw, Poland
[b] Faculty of Chemistry, University of Warsaw, PL-02-093 Warsaw, Poland
[c] Department of Molecular Sciences, Swedish University of Agricultural Sciences, P.O.Box 7015, SE-750 07 Uppsala, Sweden
[d] Wigner Research Centre for Physics, Konkoly-Thege Miklós út 29-33, H-1121 Budapest, Hungary
[e] Department of Physical Chemistry, University of Debrecen, Egyetem tér 1, H-4032 Debrecen, Hungary
[f] MAX IV Laboratory, Lund University, P.O.Box 118, SE 221 00 Lund, Sweden

## ARTICLE INFO

## ABSTRACT

At the dissolution of solid anhydrous thallium(III) trifluoromethanesulfonate, $Tl(CF_3SO_3)_3$, or thallium(III) trifluoroacetate, $Tl(CF_3COO)_3$, in dimethylsulfoxide (dmso) or $N,N,N',N'$-tetramethylurea (tmu), intensely red-colored complexes are formed. This red thallium complex is stable for years in dmso, while it is reduced fairly rapidly to thallium(I) in tmu with a half-life time of an hour. At the dissolution of $Tl(CF_3SO_3)_3$ in $N,N$-dimethylpropyleneurea (dmpu) an immediate reduction to thallium(I) takes place. A stable colorless aqueous thallium(III) solution is obtained at the dissolution in acidic water. Stable dmso solutions and solid dmso solvates of thallium(III) perchlorate, nitrate and trifluormethanesulfonate can be prepared by adding dmso to concentrated acidic aqueous thallium(III) solutions. These experimental observations conclude that the pure solids $Tl(CF_3SO_3)_3$ and $Tl(CF_3COO)_3$ play an essential role in the formation of the red-colored thallium complexes. $^{205}$Tl NMR data show that the red thallium complex contains equal amounts of thallium(III) and thallium(I). The structure of the red thallium complex in dmso, as determined by EXAFS, has Tl–O bond distances of 2.216(3) and 2.80(2) Å, which are in very close agreement with the bond distances obtained in the pure dmso solvates of the thallium(III) and thallium(I) ions, respectively, and a Tl···Tl distance of 3.49(1) Å bridged by oxygen atoms. From the EXAFS data it is impossible to distinguish if dmso molecules and/or trifluoromethanesulfonate ions act as bridges. DFT calculations could eliminate some structures due to the irrelevant structural parameters or the energetics of the proposed reactions.

## 1. Introduction

In attempts to prepare dimethylsulfoxide (dmso) solutions of thallium(III) by dissolving anhydrous thallium(III) trifluoromethanesulfonate, $Tl(CF_3SO_3)_3$, and thallium(III) trifluoroacetate, $Tl(CF_3COO)_3$, in freshly distilled dmso, intensely red-colored solutions are formed, while they become orange in dilute solution, *vide infra*. The formed complexes in dmso are stable over long periods of time, years. Contrary to this observation, a stable dmso solvated thallium(III) ion is obtained by adding a small volume of concentrated aqueous thallium(III) perchlorate solution to freshly distilled dmso [1]. Stable solid [Tl(dmso)$_6$](ClO$_4$)$_3$ crystals are obtained by evaporating this solution for

some days. The structure of the dmso solvated thallium(III) ion is a regular octahedral complex with mean Tl–O bond distances of 2.224 and 2.22 Å in solid state and dmso solution, respectively [1]. A crystal structure of [Tl(dmso)$_6$](NO$_3$)$_3$ also reports a mean Tl–O bond distance of 2.224 Å [2].

Dissolution of $Tl(CF_3SO_3)_3$ in another organic solvent, $N,N,N',N'$-tetramethylurea (tmu), also resulted in a red-colored solution, which faded away within less than a day. When $N,N,$-dimethylpropyleneurea (dmpu) is used as solvent, no red color was observed, and reduction to thallium(I) takes place instantaneously. Dissolution of $Tl(CF_3SO_3)_3$ in perchloric or trifluoromethanesulfonic acidic water results in stable colorless thallium(III) solutions. The red color observed in dmso and tmu

---

* Corresponding authors.

*E-mail addresses:* imre.toth@science.unideb.hu (I. Tóth), ingmar.persson@slu.se (I. Persson).

may indicate that a mixed-valence complex is formed as both thallium (III) and thallium(I), as $d^{10}$ and $d^{10}s^2$ metal ions, respectively, form colorless complexes separately.

The perchlorate and trifluoromethanesulfonate ions are regarded as non-coordinating ligands, and therefore, they are often used when hydrated, and solvated metal ions are studied in solution. The thallium(III) ion is hexahydrated in the solid perchlorate salt, $[Tl(H_2O)_6](ClO_4)_3$ [3], as well as in aqueous solution [4,5]. On the other hand, with trifluoromethanesulfonate as counter ion, thallium(III) forms a neutral complex binding three water molecules and three trifluoromethanesulfonate ions in solid state, $[Tl(H_2O)_3(OSOCF_3)_3]$ [6]. The isoelectronic mercury(II) ion displays a similar pattern in solid state by forming a hexahydrate with perchlorate, $[Hg(H_2O)_6](ClO_4)_2$ [7]. With trifluoromethanesulfonate as counter ion, a polymeric hydrated mercury(II) compound is formed, $[Hg(H_2O)_2(OSO_2CF_3)_2]_\infty$ [6]. This indicates significant interactions between thallium(III) and trifluoromethanesulfonate ions, and may impact the formation of the red-colored thallium complex.

The coordination chemistry of thallium(I) in solution is less explored than thallium(III) due to the weak bonds thallium(I) forms. No hydrate but a couple of thallium(I) solvate complexes have been reported in solid state [8]. Two examples are tris(4-nitrophenoxo)-thallium(I) 4-nitrophenolate [9] and tetrakis(diethylether)thallium(I) bis(tris(pentafluorophenyl)borato)ammonium[10] with O–Tl–O bond angles in the range 72.4–123.4 and 86.8–133.3°, respectively. All thallium(I) compounds characterized crystallographically show a significant gap in the coordination sphere [8]. A structure study of the hydrated and dmso solvated thallium(I) ions in solution showed very weak Tl–O bonds in the region 2.8–3.2 Å, but it was not possible to describe any geometric coordination figure [11]. $^{205}$Tl NMR has been shown to be a sensitive tool to determine the solvation strength of thallium(I) in solvents [12]. The $^{205}$Tl NMR shifts of thallium(I) in a series of solvents have a linear correlation with the donor strength scale, $D_S$ [13], showing the soft binding character of thallium(I), Fig. S1.

The coordination chemistry of thallium(I) is expected to be strongly influenced by its electron configuration, $5d^{10}6s^2$. The tendency of the heavier main group elements to adopt an oxidation state two steps below being fully oxidized was originally attributed to the effect of the so-called "inert electron-pair" [14] connected with the relativistic stabilization of the 6s orbital, caused by the direct relativistic effect and the presence of the filled 4f subshell. According to the valence bond theory, the inert electron-pair can either occupy a hybrid orbital formed by mixing the 6s and 6p orbitals on the metal ion and becomes stereochemically active, or be a pure $s^2$ electron-pair and thereby stereochemically inactive. The hybrid orbital with a lone electron-pair can, in terms of coordination number, be considered as at least an additional ligand in the coordination sphere, normally taking up more space than that of an ordinary ligand [15,16]. However, according to molecular orbital theory, the classical concept of 6s/6p orbital hybridization on the isoelectronic lead(II) ion is regarded as incorrect as the energy levels of these orbitals are too different and have very different spatial distribution of their wave-functions [17–20]. This should certainly also apply to the isoelectronic thallium(I) ion as it displays a similar kind of coordination chemistry as lead(II) and bismuth(III). The strong stereochemical activity observed in a large number of lead(II) and bismuth (III) complexes must instead be a result of an anti-bonding metal 6s-ligand np (6s/np) interaction which causes structural distortions to energetically minimize these unfavorable covalent interactions [18–21]. It can therefore be assumed that thallium(I) also forms a huge gap in its coordination sphere, as seen in the few examples mentioned above.

A light-sensitive mixed-valence thallium(III)-thallium(I) porphyrin complex has been reported [22]. In this complex thallium(III) is bound to nitrogens in a porphyrin core, while thallium(I) is attached to a side-chain. This complex was formed at exposure to indirect sunlight, and dissociates in direct sunlight, and does not show the stability the mixed valence thallium(III)-thallium(I) complex reported in this study has.

The aim of this study is to get a deeper understanding of the oxidation state(s) and structure of the red-colored thallium complexes formed at the dissolution of solid $Tl(CF_3SO_3)_3$ and $Tl(CF_3COO)_3$ in dmso and tmu. A series of physico-chemical and structural studies on solutions with dissolved $Tl(CF_3SO_3)_3$ have been performed in water, dmso, dmpu, and tmu. The structure and the oxidation states of the red thallium complexes in dmso and/or tmu have been determined by $^{205}$Tl-NMR, X-ray absorption spectroscopy, and cyclic voltammetry. Electronic spectra have been recorded to characterize the red complex in the tmu solution and to follow the spontaneous reduction of the red thallium complex in this solvent. The experimental studies on dmso solutions of the red thallium complex have been complemented with DFT simulations to find the most stable structure of a mixed valence thallium(III)-thallium (I) complex with trifluoromethanesulfonate as a counter ion. Despite the highly poisonous properties of thallium, its compounds are still a curious research object [23–26]. The possibility of thallium occurring in two oxidation states with very different coordination chemistry, makes its connections for structural and materials studies interesting [27–31]. The redox processes between the two oxidation states of thallium are also eagerly studied [32,33]. However, potential applications such as using thallium(III) complexes as radiopharmaceuticals or chemotherapeutics to fight cancer may be particularly essential [34,35].

## 2. Experimental

### 2.1. Chemicals

**Solvents.** Dimethylsulfoxide, $(CH_3)_2SO$ (dmso, Merck), *N,N'*-dimethylpropyleneurea, $(CH_2)_3(N(CH_3))_2CO$ (dmpu, BASF) and *N,N,N',N'*-tetramethylurea, $((CH_3)_2N)_2CO$ (tmu, Chemicon) were distilled over calcium hydride, $CaH_2$, (Fluka) immediately before use.

**Salts.** *Thallium(III) trifluoromethanesulfonate, $Tl(CF_3SO_3)_3$,* was prepared as described elsewhere [1]. *Thallium(I) trifluoromethanesulfonate, $TlCF_3SO_3$,* was prepared by dropwise addition of trifluoromethanesulfonic acid (Fluka) to an aqueous slurry of *thallium(I) carbonate,* $Tl_2CO_3$, (Sigma-Aldrich, 99%) until a clear solution was obtained. This solution was filtered, and finally excess water and trifluoromethanesulfonic acid were boiled off in an oven at 450 K. Thallium(I) and thallium(III) trifluoromethanesulfonate are white powders, which were stored in an oven at 450 K to minimize the uptake of water. A much faster preparation route of *hexakis(dmso)thallium(III) nitrate, $[Tl(OS(CH_3)_2)_6](NO_3)_3$,* than reported in ref. 2 can be made by adding dmso to saturated thallium(III) nitrate in 10 mol·dm$^{-3}$ nitric acid resulting in a pale yellow precipitate. In an attempt to prepare *hexakis (dmso)thallium(III) trifluoromethanesulfonate, $[Tl(OS(CH_3)_2)_6](CF_3SO_3)_3$,* in the same way as the nitrate and perchlorate salts resulted in white milky precipitation. Most importantly, by using this preparation procedure no red mixed-valence complex was formed.

**Preparation of solutions.** Weighed amounts of dry $Tl(CF_3SO_3)_3$ or $TlCF_3SO_3$ were dissolved in the respective solvent to the concentration applied in the different experiments, see text below.

### 2.2. Experimental methods

#### 2.2.1. UV–Vis spectrophotometry

Electronic absorption spectra were recorded in the range 200–700 nm with a scan rate of 200 nm/min on a double beam Thermo Scientific Evolution 600 UV–Vis spectrometer. The spectra were collected using quartz cuvettes with a 1 cm path length.

**$^{205}$Tl NMR.** $^{205}$Thallium-NMR spectra were measured at 8.46 Tesla, on a Bruker Avance I 360 MHz spectrometer using a (home modified) 5 mm BB probe tuning the BB-channel to the frequency of $^{205}$Tl, 207.74 MHz. The probe temperature was kept at 25.0 ($\pm$0.1) °C. Thallium chemical shifts were referenced externally to infinitely diluted $TlClO_4$ in water as 0 ppm, using 50 mM thallium(I)- and thallium(III)-perchlorate solutions, $Tl^+$: $-4.72$ ppm and $Tl^{3+}$: 2039 ppm for $^{205}$Tl and $^{203}$Tl

spectra. Typical instrument parameters were used, $TD = 16$ K, $SW = 150$– $360$ ppm, $p1 = 12.6$ μs $(45°)$, $d1 = 1.5$–$3$ s, with 8–256 transients. $^{205}$Tl longitudinal relaxation time constants $(T_1)$ were determined at room temperature by an inversion recovery experiment ($\pi$-delay-$\pi/2$ pulse sequence) in pseudo 2D mode provided with the Bruker Avance I 360 MHz spectrometer. The results were calculated by a non-linear parameter fitting using the TopSpin© software (Bruker AG) [36].

### 2.2.2. EXAFS spectroscopy

Thallium L$_3$ edge X-ray absorption data were collected in transmission mode at the Balder beamline at the MAX IV synchrotron light facility, Lund University, Sweden [37,38], and at Stanford Synchrotron Radiation Laboratory (SSRL), wiggler beamline 4–1 (old station). At MAX IV, spectra were acquired using a continuous scan scheme, where the Bragg axis as well as the vertical beam offset are moved simultaneously with constant velocity to fix the vertical position of the beam [38], while data collection at SSRL was performed in step scan mode. The radiation was monochromatized by Si(111) double crystal monochromators. The solutions were contained in sample cells made of a 3.0 mm Teflon spacer and Kapton foil windows hold together with titanium frames. The XAS spectra recorded at the Balder beam-line were measured in continuous energy scanning mode at a speed of 50 sec/full EXAFS spectrum ($k_{max} = 14.5$ Å$^{-1}$). The monochromatic flux at the sample was $\sim 10^{12}$ photons/sec with a spot size of approximately 0.10 (horizontal) $\times$ 2.0 (vertical) mm$^2$. For each sample, 20 repeats were examined for possible radiation damage and afterwards accumulated into an average spectrum. Immediately before the start of each repeat, the sample was shifted by 0.20 mm into a fresh position to avoid radiation dose accumulation. In general, only a single EXAFS scan was recorded on each sample position. The energy axis was calibrated with repeated spectra of a selenium foil with first inflection point assigned as 12658 eV, which is identical to the energy of the L$_3$ edge of metallic thallium [39]. The EXAFSPAK program package was used for the data treatment [40]. The EXAFS oscillations were extracted using standard procedures for pre-edge subtraction, spline removal and data normalization. Model fitting, including both single and multiple back-scattering pathways, was performed with theoretical phase and amplitude functions calculated *ab initio* by means of the computer code FEFF7 [41]. The $k^3$-weighted EXAFS oscillation was analyzed by a non-linear least-squares fitting procedure.

### 2.2.3. Cyclic voltammetry

Electrochemical experiments were performed using a CHI 650D electrochemical workstation (CHI Instruments Inc., Austin, Texas, USA). A conventional three-electrode system with a non-aqueous Ag/AgCl electrode in tetrabutylammonium chloride/methanol with a double junction was used as the reference electrode. This secondary salt bridge was filled with the electrolyte solution used in the experiments. A platinum foil was used as the counter electrode and the glassy carbon electrode (GCE) of 3 mm diameter (GCE, BASi® West Lafayette, Indiana, USA) as the working electrode. All experiments were performed at 25 °C in 0.2 mol·dm$^{-3}$ tetra-*n*-butylammonium trifluoromethanesulfonate (($n$-C$_4$H$_9$)$_4$N(CF$_3$SO$_3$)) in dry tmu as the supporting electrolyte. The reference electrode was calibrated using the process of ferrocene oxidation in the same ($n$-C$_4$H$_9$)$_4$N(CF$_3$SO$_3$)/tmu solution. During the experiment, argon was used to deaerate the solution, and an argon blanket was maintained over the solution. The GC electrode was polished mechanically with 1.0, 0.3 and 0.05 μm alumina powder on a Buehler polishing cloth to a mirror-like surface and rinsed with water and dmso.

### 2.3. DFT methods

Density Functional Theory (DFT) calculations have been carried out using the Gaussian09 software package [42]. Geometry optimizations have been performed with the M06 functional [43]. TZVP basis sets [44] for the non-metal elements while CRENBL ECP and the related basis sets

are used for the thallium atoms [45]. Frequency calculations have been done at the theoretical level of geometry optimization. Relative free energies ($\Delta G$) are reported at 298.15 K and atmospheric pressure. The solvent effect is accounted for the Integral Equation Formalism Polarized Continuum Model (IEF-PCM) [46]. All stationary points, minima and transition states (TS) have been proven by frequency analysis where minima have all positive frequencies, and TSs have one imaginary frequency related to the actual movement of the reaction coordinate. All energies are given in kJ·mol$^{-1}$.

## 3. Results and discussion

### 3.1. Structure of solid anhydrous thallium(III) trifluoromethanesulfonate, $Tl(CF_3SO_3)_3$

The XANES spectrum of solid anhydrous thallium(III) trifluoromethanesulfonate, Tl(CF$_3$SO$_3$)$_3$, is in very close agreement with those of aqueous and dmso solutions of thallium(III), Fig. 1a. Refinement of the EXAFS data reveals a Tl–O bond distance of 2.205(2) Å, and a multiple TlO$_6$ scattering pattern strongly indicating regular octahedral coordination. The mean Tl–O-S bond angle was determined to 149(2)°. The fits of the raw EXAFS data and the Fourier transform are given in Fig. S2, and the refined structure parameters in Table S1. The Tl–O bond distance in Tl(CF$_3$SO$_3$)$_3$ is in close agreement with other octahedral thallium(III) complexes/compounds, Table S2. As no Tl···Tl distance was observed in the EXAFS study of solid Tl(CF$_3$SO$_3$)$_3$, Table S1 and Fig. S2, the shortest Tl···Tl distance is certainly longer than 5–6 Å. Thereby, it seems likely that thallium(III) binds to different oxygens in bridging trifluoromethanesulfonate ions.

### 3.2. Conditions for the formation of red thallium complexes

Red-colored mixed valence thallium(III)-thallium(I) complexes form at the dissolution of solid anhydrous Tl(CF$_3$SO$_3$)$_3$ and Tl(CF$_3$COO)$_3$ in dmso and tmu. The addition of water to such solutions does not alter the color. A stable colorless aqueous thallium(III) solution is obtained at the dissolution of Tl(CF$_3$SO$_3$)$_3$ in acidic water. On the other hand, at the dissolution of solid Tl(CF$_3$SO$_3$)$_3$ in dmpu, an instantaneous reduction to thallium(I) takes place. The dmso solvated thallium(III) ion is stable in both solution and solid state with perchlorate and nitrate as counter ions [1,2], as well as for trifluoromethanesulfonate when it is prepared by the addition of dmso to saturated aqueous thallium(III) solution in highly concentrated trifluoromethanesulfonic acid. Furthermore, no visible reaction occurs when dmso solutions with equimolar amounts of thallium(III) perchlorate and thallium(I) trifluoromethanesulfonate are mixed, and neither when an excess sodium trifluoromethanesulfonate is
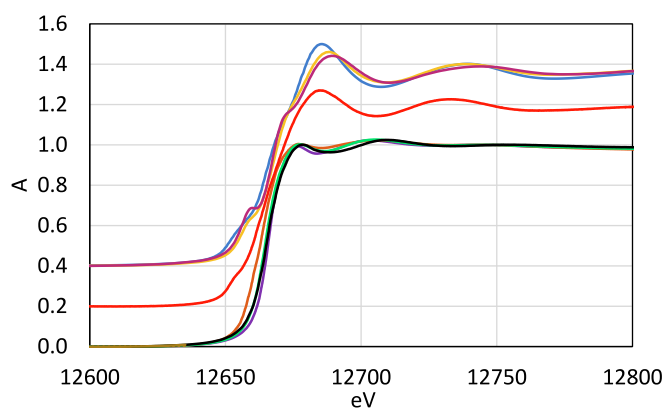


**Fig. 1a.** XANES spectra of thallium(I) in aqueous (purple line), dmso (black line), tmu (green line) and dmpu (brown line) solution, no offset, red thallium (red line), offset: 0.2, and thallium(III) in aqueous (dark blue line) and dmso (yellow line) solution and solid Tl(CF$_3$SO$_3$)$_3$ (cerise line), offset: 0.4.

added. The experimental observations described above show that the red-colored thallium complexes form only when *anhydrous* thallium(III) trifluoromethanesulfonate or trifluoroacetate are dissolved in dmso or tmu. The key factors for the formation of the red thallium complex seem to be that thallium(III) must be coordinated by a counter ion bridging other thallium(III) ions, and that the solvent has well tuned reducing and coordination ability to stabilize the mixed-valence thallium(III)-thallium(I) complex. Dmso seems to be more or less perfectly tuned for this system, while tmu, and especially dmpu, are too strong reducing agents. On the other hand, water is too weak as a reducing agent to reduce thallium(III) in $Tl(CF_3SO_3)_3$ to thallium(I).

### 3.3. Determination of oxidation states of thallium in red thallium complexes

#### 3.3.1. $^{205}Tl$ NMR

A $^{205}Tl$ NMR spectrum of a red thallium dmso solution stored for three months at room temperature shows two signals attributed to thallium(III) and thallium(I), at chemical shifts of 2010 and 475 ppm, respectively, see Table 1. The intensity ratio of the two signals is 0.97, i. e. the thallium(III)/thallium(I) concentration ratio is close to 1:1 with a small excess of thallium(I). As the sample has been prepared to form at 0.20 $mol·dm^{-3}$ $Tl(CF_3SO_3)_3$ solution, the concentration of a dimeric mixed valence complex is *ca.* 0.10 $mol·dm^{-3}$. As the thallium(III)/thallium(I) ratio is close to one in the red thallium complex it clearly indicates a redox reaction between the thallium(III) and dmso, which most likely stops due to the stability of the mixed valence thallium(III)-thallium(I) complex. Two signals with equal intensity might be attributed to a mixture of thallium(III) and thallium(I) or to a compound with thallium(III) and thallium(I) in 1:1 ratio. The chemical shift values of $Tl(dmso)_6^{3+}$ and $Tl(dmso)_x^+$ in dmso solution are known from our earlier studies; 1886 and 361 ppm in the presence of perchlorate as counter anion, respectively [1]. The differences of +124 and +114 ppm, respectively, are not dramatic considering the large chemical shift scale of $^{205}Tl$ NMR, and the sensitivity of the chemical shift to concentration, counter ion, solvent (purity), temperature etc. [12]. In addition, the absence of scalar spin–spin coupling between closely located Tl-atoms $<$(Tl–O–Tl, i.e. $^2J_{(Tl-Tl)}$) does not support the formation of a complex containing both thallium(III)-thallium(I). However, we do not know and cannot predict the $^2J_{(Tl-Tl)}$ value in the case of a thallium(III)-thallium(I) entity bridged with one or several O-atom(s). $^2J_{(Tl-Tl)}$ values measured for thallium(III)-thallium(III) coupling ranges 800 Hz and 2700 Hz in

two polyoxometallates (POM) containing two Tl-atoms. However, no data are published for the thallium(I)-thallium(III) interaction, and this coupling constant could be much smaller, even unmeasurable [47,48].

The interaction of thallium(III) and thallium(I) might affect the longitudinal relaxation time constant ($T_1$) of the thallium(III) and thallium(I) signals. Therefore, the $T_1$ values in the "red thallium" sample at 8.46 Tesla have been measured to 223 and 380 ms, respectively. For comparison, we have also determined $T_1$ of $Tl(dmso)_6^{3+}$ and $Tl(dmso)_x^+$ in the presence of perchlorate anion in separated samples ($c_{Tl} = 0.02$ $mol·dm^{-3}$); the measured values are 291 and 287 ms, respectively. These time constants are slightly smaller than the $T_1$ value measured for the aqueous $Tl(H_2O)_6^{3+}$ ion ranging from 310 to 2020 ms, depending on the acid content, ionic medium, and magnetic field strength [49]. Interestingly, after mixing thallium(III) and thallium(I) ($c_{Tl(III)} = c_{Tl(I)} = 0.01$ $mol·dm^{-3}$, perchlorate counter anion), the measured $T_1$ values in this colorless solution are somewhat (although not dramatically) different from the values measured in "pure" samples, 245 ms and 501 ms, respectively. This solution remains colorless after adding $KCF_3SO_3$ salt to the solution. The chemical shift of thallium(I) is slightly changed, while the chemical shift of thallium(III) is not affected. At the same time, the $T_1$ values for both thallium(I) and thallium(III) are shortened significantly, indicating some interaction between the $CF_3SO_3$ anion and both thallium(I) and thallium(III). A dmso solution containing thallium (I), thallium(III) and dimethylsulfone, likely the product of oxidation of dmso by thallium(III) in the "red thallium" sample, but neither any color-change, nor a chemical shift change indicate any role of dimethylsulfon. In the case of the above mentioned Tl-containing POM, $[Tl_2Na_2(H_2O)_2(P_2W_{15}O_{56})_2]^{16-}$, the measured $T_1 = 22$ ms for $^{205}Tl$ longitudal relaxation time of thallium(III) is substantially shorter compared to the actual 75–500 ms values measured in dmso solution [38]. The large decrease in the POM can likely be attributed to the strong Tl-Tl interaction and different chemical shift anisotropy (CSA) mechanism instead of a spin-rotation mechanism suggested for a thallium(III) ion with non-distorted $O_h$ symmetry in a small molecule [49].

$^{205}Tl$ NMR experiments show that the dissolution of solid $Tl(CF_3SO_3)_3$ or $Tl(CF_3COO)_3$ in dmso results in stable red-colored solutions with half of the thallium(III) reduced to thallium(I). The experimental NMR parameters, neither the chemical shift values nor the $T_1$ time constants of the"red Tl sample", show any significant differences compared to a colourless dmso solution prepared by dissolving thallium (I) and thallium(III) salts in equimolar amounts.

#### 3.3.2. XANES

X-ray absorption near-edge structure (XANES) spectra at the Tl $L_3$-edge were collected on a two-day old red thallium dmso solution, and of $TlCF_3SO_3$ dissolved in water, dmso, tmu and dmpu, and previously reported XANES spectra of thallium(III) perchlorate in aqueous and dmso solution [1] are shown in Fig. 2a. The XANES spectra of thallium(I) are similar without any features on the edge and an edge position at about 12665 eV; the XANES spectra of thallium(I) are plotted with offset for better visibility in Figure S3. The absorption edge position of the solvated thallium(I) follows nicely the reversed order of the electron-pair donor ability [13] and $^{205}Tl$ NMR shift [12], Fig. S1, showing the soft bonding character of thallium(I). The XANES spectra of thallium(III) have two pronounced shoulders on the absorption edge with inflection points at 12655 and 12671 eV, and a weak white-line peaking at *ca.* 12685 eV. Red thallium has a XANES spectrum in between thallium(I) and thallium(III), but there are significant differences between the XANES spectrum of the red thallium complex in dmso and the mean spectrum (1:1) of the spectra of thallium(III) and thallium(I) in dmso, Fig. 1b. Especially, the first shoulder on the absorption edge appears at significantly lower energy than both thallium(I) and thallium(III). This shows that the red thallium complex is different from the mean of the solvated thallium(I) and thallium(III) ions in dmso solution, and thereby not a mixture of separate dmso solvated thallium(III) and thallium(I) ions.

**Table 1**
$^{205}Tl$ NMR parameters of thallium(I) and thallium(III) in dmso solutions.

| Species | Anion | Shift $Tl^I$/ ppm | Shift $Tl^{III}$/ ppm | $T_1$ $Tl^I$/ ms | $T_1$ $Tl^{III}$/ ms | Ref. |
|---|---|---|---|---|---|---|
| $Tl^+$/dmso | $ClO_4^-$ | 361 | – | – | – | 1 |
| $Tl^+$/dmso | $ClO_4^-$ | 360 | – | 287 | – | This work |
| $Tl^{3+}$/dmso | $ClO_4^-$ | – | 1886 | – | – | 1 |
| $Tl^{3+}$/dmso | $ClO_4^-$ | – | 1885 | – | 291 | This work |
| $Tl^+ + Tl^{3+}$/ dmso [a] | $ClO_4^-$ | 360 | 1883 | 501 | 245 | This work |
| $Tl^+ + Tl^{3+}$/ dmso [b] | $ClO_4^- + CF_3SO_3^-$ | 351 | 1883 | 343 | 75 | This work |
| $Tl^+ + Tl^{3+}$/ dmso [b] | $ClO_4^- + CF_3SO_3^-$ + 0.1 M dimethyl sulfone | 335 | 1879 | 345 | 90 | This work |
| $Tl^{3+}$/dmso [c] | $ClO_4^- + CF_3SO_3^-$ | | 1881 | – | – | This work |
| Red thallium | $CF_3SO_3^-$ | 474 | 2012 | 380 | 223 | This work |

[a] $c(Tl^+) = c(Tl^{3+}) = 0.01$ M, $c(ClO_4^-) = 0.04$ M; [b] $c(Tl^+) = c(Tl^{3+}) = 0.1$ M, $c(ClO_4^-) = 0.4$ M, $c(CF_3SO_3^-) = 0.3$ M; [c] $c(Tl^{3+}) = 0.1$ M, $c(ClO_4^-) = 0.3$ M, $c(CF_3SO_3^-) = 0.3$ M.
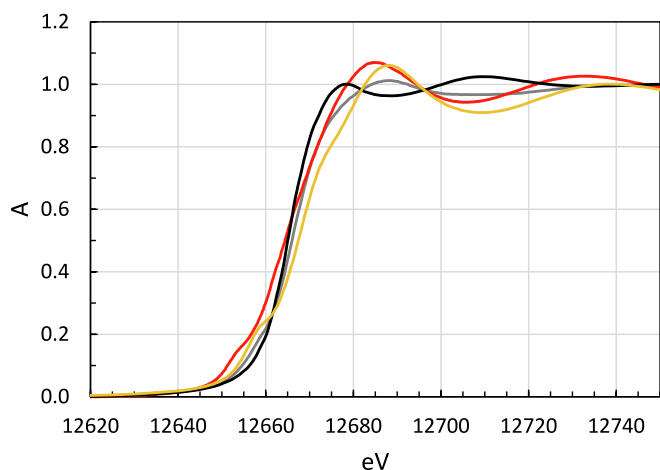
**Fig. 1b.** XANES spectra of thallium(I) trifluoromethanesulfonate in dmso solution (black line), thallium(III) perchlorate in dmso solution (yellow line), red thallium dmso solution formed at dissolution of solid Tl(CF₃SO₃)₃, (red line), and the mean of the thallium(I) and thallium(III) dmso solutions (grey line).
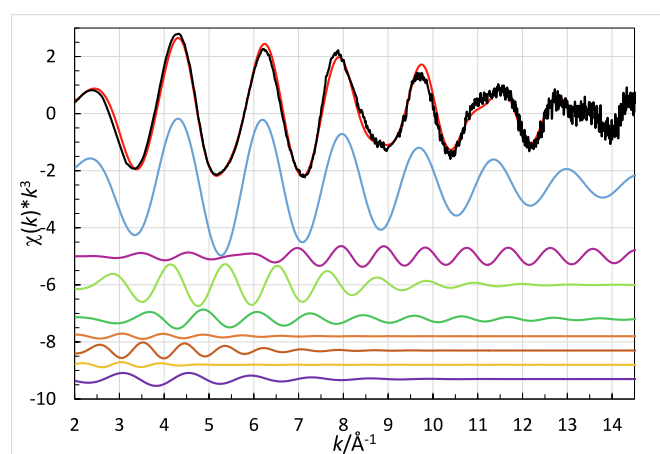


**Fig. 2.** Fit of raw EXAFS data of red thallium in dmso solution, black line – experimental data, and red line calculated EXAFS function the parameters given in Table 2. The individual contributions to the applied model are Tl$^{III}$-O, single scattering (SS) – light blue line, offset: −2.5, Tl$^{III}$···Tl$^{I}$ SS – cerise line, offset: −5.0, Tl$^{III}$···S, SS – light green line, offset: −6.0, Tl$^{III}$-O-S three leg scattering – green line, offset: −7.2, linear multiple scattering within Tl$^{III}$O₆ entity, light brown, brown and orange lines, offsets: −7.8, −8.3 and 8.8, and Tl$^{I}$-O, SS – purple line, offset: −9.3.

### 3.3.3. EXAFS study of the red thallium complex in dimethylsulfoxide

The information obtained from XANES and $^{205}$Tl NMR spectra show that the red thallium dmso solution contains both thallium(I) and thallium(III), and it is different from the mean of individual solvated thallium(III) and thallium(I) ions, *vide ultra*. It is clearly seen in the high *k* part of the EXAFS function of the red thallium complex that there are two strong contributions. The only reasonable contributions at *k* > 11 Å⁻¹ are Tl$^{III}$-O and Tl···Tl single scattering. A model with an octahedral geometry around a thallium(III) site which bridges through two oxygens to a thallium(I) site with a Tl···Tl distance of 3.49(1), and mean Tl–O bond distances of 2.216(3) and 2.80(3) Å to the thallium(III) and thallium(I) sites, respectively, has been applied, Table 2. The observed Tl$^{I}$-O and Tl$^{III}$-O bond distances are in full agreement with the structures of the dmso solvated thallium(III) and thallium(I) ions, respectively [1,11]. The mean Tl$^{III}$-O-S bond angle is determined to 120° from the Tl···S single and the Tl–O-S three-leg scattering paths, which is in full agreement with structures of the dmso solvated thallium(III) ion in solid state

**Table 2**
Mean bond distances, *d*/Å, Debye-Waller factors, σ²/Å², number of distances, *N*, the threshold energy, $E_o$/eV, the amplitude reduction factor, $S_o^2$, and the goodness of fit, *F*, as defined in ref. 26, of the studied red thallium complex in dmso in the *k* range 2–15 Å⁻¹ at ambient room temperature.

| Solvent Interaction | N | d | σ² | $E_o$ | $S_o^2$ | F |
|---|---|---|---|---|---|---|
| *Tl(CF₃SO₃)₃ in dmso solution (red thallium)* | | | | | | |
| Tl$^{III}$-O | 3 | 2.216(1) | 0.0058(1) | 12688.4(2) | 0.84(1) | 19.9 |
| MS (TlO₆) | 3*3 | 4.433(2) | 0.021(1) | | | |
| Tl$^{III}$···S | 3 | 3.275(5) | 0.0176(9) | | | |
| Tl$^{III}$-O-S | 6 | 3.481(12) | 0.0083(8) | | | |
| Tl···Tl | 1 | 3.490(3) | 0.0080(2) | | | |
| Tl$^{I}$-O | 2 | 2.80(2) | 0.023(3) | | | |

and dmso solution [1]. The refined structure parameters are summarized in Table 2, and the fit of the experimental EXAFS raw data together with individual contributions of the applied model are shown in Fig. 2.

### 3.3.4. DFT simulations

The starting point in the DFT simulation is the results from the EXAFS study of the red Tl dmso solution summarized in Table 2. The different Tl$^{I}$-O and Tl$^{III}$-O bond distances can be attributed to an adduct formed from solvated thallium(I) and thallium(III) entities bridged by two μ-O atoms of dmso molecules and/or trifluoromethanesulfonate ions. The formation of the complex is basically concluded from the relatively short Tl···Tl distance at 3.49 Å observed by EXAFS. Studying the possible forms of the "Tl$^{I}$–Oₓ-Tl$^{III}$" complex by DFT calculations, structures with only dmso ligands including bridging ones or with dmso and CF₃SO₃⁻ anion(s) both in bridging and terminal positions either at thallium(I) or thallium(III) have been considered. The anion certainly plays a crucial role in the redox reaction during the reduction of thallium(III) to thallium(I), and it might decrease the obviously strong electrostatic repulsion between the + 1 and + 3 charged cations in the proposed mixed-valence thallium(III)-thallium(I) complex.

The [(dmso)₃Tl$^{I}$···Tl$^{III}$(dmso)₆]$^{4+}$ and [(dmso)₂(CF₃-SO₃) Tl$^{I}$···Tl$^{III}$(dmso)₆]$^{3+}$ complexes have several isomers. However, there are only two structural types with low energy showing fairly good agreement with the structural parameters calculated from the experimental EXAFS data, Fig. 3 (see Table 2 and with bond angles described *vide ultra*).

In the case of the [(dmso)₃Tl$^{I}$···Tl$^{III}$(dmso)₆]$^{4+}$ species (**1**), there is a weak interaction between thallium(I) and one of the sulfur atoms (3.42 Å), the following structural parameters have been calculated including two bridging dmso molecules: Tl···Tl 3.48 Å, Tl$^{I}$–O1$_{dmso}$ 2.76 Å, Tl$^{I}$–O2$_{dmso}$ 2.81 Å, O1$_{dmso}$–Tl$^{I}$–O2$_{dmso}$ 64°, mean Tl$^{III}$–O 2.27 Å, Tl$^{I}$–O1$_{dmso}$–Tl$^{III}$ 87° and Tl$^{I}$–O2$_{dmso}$–Tl$^{III}$ 85°. In the case of the [(dmso)₂(CF₃-SO₃)Tl$^{I}$···Tl(dmso)₆]$^{3+}$ complex isomer (**2**) the following structural parameters including again two bridging dmso molecules can be distinguished: Tl–Tl 3.47 Å, Tl$^{I}$–O1$_{dmso}$ 2.75 Å and Tl$^{I}$–O2$_{dmso}$ 2.74 Å, O1$_{dmso}$–Tl$^{I}$–O2$_{dmso}$ 65°, both Tl$^{I}$–O1$_{dmso}$–Tl$^{III}$ and Tl$^{I}$–O1$_{dmso}$–Tl$^{III}$ 87°. In **2** there is also a weak Tl$^{I}$–S bond (3.48 Å), while the CF₃-SO₃⁻ ligand is coordinated by two oxygen atoms, however, one of them has a shorter Tl–O distance. The Gibbs free energy of the reaction **1** + CF₃SO₃⁻ ⇌ **2** + dmso is –20.6 kJ mol⁻¹ predicting the dominant existence of **2** (almost 100%). The binding of a trifluoromethanesulfonate ion to the thallium (I) site is supported by $^{205}$Tl NMR measurements with excess potassium trifluoromethanesulfonate, *vide ultra*.

It is important to note that those [(dmso)₃Tl$^{I}$···Tl(CF₃SO₃)(dmso)₅]$^{3+}$ complexes, where the CF₃SO₃⁻ ligand is located in a terminal position on thallium(III) or in a bridging position, have higher energies (+18–27 kJ mol⁻¹) than **2** and the Tl···Tl distance shows a wide variety (3.28, 3.53 or 4.08 Å). These species (**5**, **6** and **7**) can be seen in Fig. S4. With two or

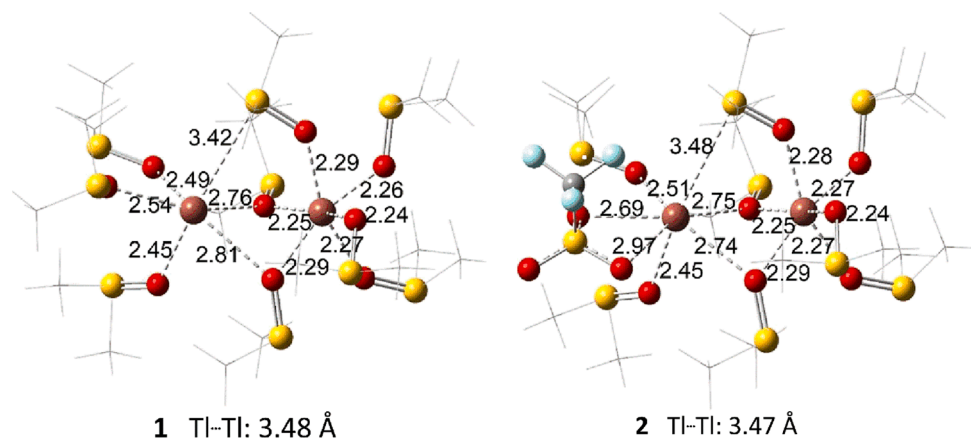**1**  Tl··Tl: 3.48 Å          **2**  Tl··Tl: 3.47 Å

**Fig. 3.** The optimized structures of **1** and **2** with the Tl–O and Tl–S distances (Å).

three $CF_3SO_3^-$ ligands binding to $Tl^I$ initiated a significant lengthening of the Tl···Tl distance to 3.75–4.25 Å.

From the geometrical point of view, in both DFT calculated complexes **1** and **2**, the thallium(III) center has rather a distorted trigonal antiprismatic geometry than a distorted octahedral one, while the [Tl(dmso)$_6$]$^{3+}$ complex exists in a slightly distorted octahedral geometry calculated by DFT. The [Tl(dmso)$_6$]$^+$ has a capped octahedral ($C_{3v}$) geometry where the gap in the coordination sphere is an anti-bonding orbital as discussed in the Introduction section.

Simulated UV–Vis spectra of complexes **1** and **2** show a maximum in absorbance around 465 nm, which is in agreement with the recorded UV–vis spectra even though it is not displaying a Gaussian shape, most likely due to the high absorbance, Figs. S5 and S6. Neither [Tl(dmso)$_x$]$^+$ nor [Tl(dmso)$_6$]$^{3+}$ has an absorption in the visible region, while both **1** and **2** have a quite intensive absorption band around 465 nm as also observed experimentally. In summary, it can be declared that the DFT and TDDFT calculations propose the existence of a [(dmso)$_2$(CF$_3$-SO$_3$)Tl···Tl(dmso)$_6$]$^{3+}$ complex there most likely the trifluoromethylsulfonate ligand coordinates to the thallium(I) ion.

### 3.3.5. Kinetics of the reduction of the red thallium complex in tmu

The kinetics of the reduction of the red thallium complex has been followed by XANES spectroscopy, UV–Vis spectrophotometry and cyclic voltammetry. XANES spectra of the red thallium complex in tmu were collected during 135 min to follow the spectral changes, and additional spectra were collected after 6 and 24 h when the decomposition of the red thallium complex was assumed to be completed, Fig. 4. The
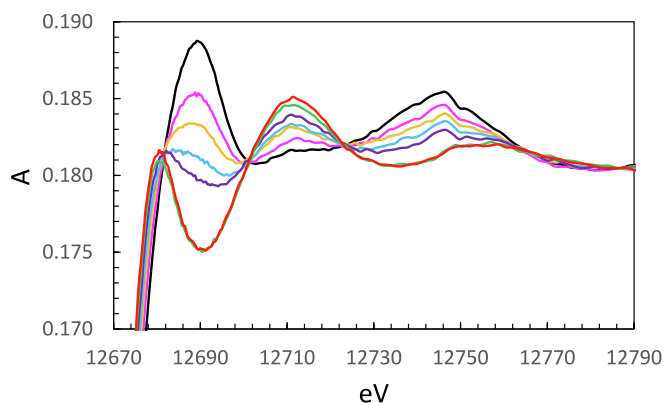
reduction reaction clearly follows first order kinetics with a half-life time of 63 ± 3 min, Fig. S7.

In general, the UV–Vis spectrum of the thallium(III) triflate solution in tmu displays intense absorption in the range of 300–500 nm without a clear point to which the maximum absorbance value can be attributed, Fig. 5. For comparison, the pure tmu spectrum shows strong absorption up to approximately 300 nm. A gradual disappearance of the presented thallium(III) spectrum can be observed in time as shown in Fig. 5, and after about 24 h from the preparation of the solution, its spectrum becomes similar to that obtained for the pure solvent. The half-life time ($t_{1/2}$) of the studied system can be estimated assuming a logarithmic disappearance of its concentration, Fig. S8. From the slopes of the marked straight lines, the estimated $t_{1/2}$ values are equal to 52.1, 51.3, 50.2, 49.5 and 48.5 min for 410, 420, 430, 440 and 450 nm, respectively, giving an average value of 50 min for these five wavelengths.

In turn, in the cyclic voltammetry studies, two peaks in the reduction half-cycle and one peak in the oxidation part were observed after dissolving thallium(III) trifluorosulfonate in tmu, Fig. 6a. The smaller and wider peak at a positive value of potential (at *ca.* +0.13 V) is responsible for reduction process: thallium(III) to thallium(I) while the higher but narrower peak at a negative value of potential (at *ca.* –0.81 V) is caused by the reduction process: thallium(I) to thallium(0). Only one peak originating from the oxidation of thallium(0) to thallium(I) was registered in the oxidation half-cycle at approximately –0.58 V. For the solution of thallium(I) trifluorosulfonate in tmu, the peak at +0.13 V was
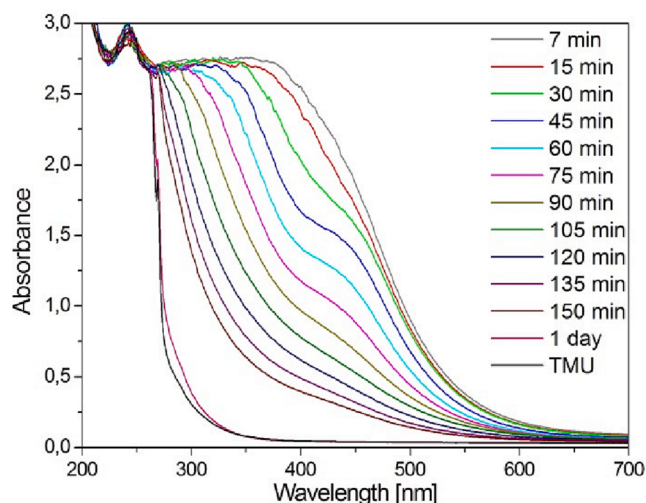


**Fig. 4.** XANES raw data of a 0.2 mol·dm$^{-3}$ tmu solution collected 35 min after the dissolution of Tl(CF$_3$SO$_3$)$_3$ (black line), after 60 min. (pink line), 85 min. (orange line), 110 (light blue), 135 min. (purple line), 6 h (green line) and 24 h (red line).



**Fig. 5.** Time evolution of UV–Vis absorption spectra for *ca.* 10$^{-3}$ M solution of Tl(CF$_3$SO$_3$)$_3$ in tmu (recorded at 15 min intervals beginning from the second spectrum; the first spectrum was recorded after 7 min).
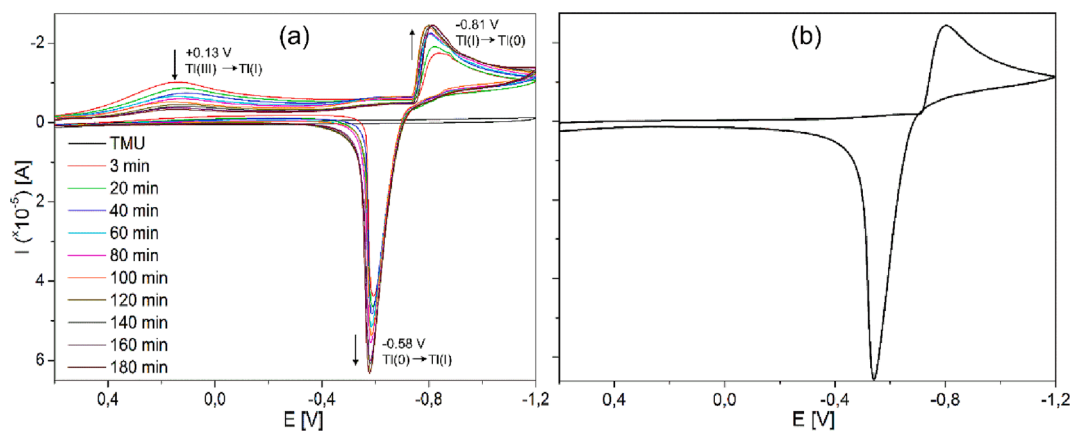
**Fig. 6.** (a) Time evolution of cyclic voltammetry curves (recorded at 20 min intervals; the first curve after 3 min, the second after 20 min) for the *ca.* $10^{-3}$ M solution of Tl(CF$_3$SO$_3$)$_3$ in tmu/0.2 M ($n$-C$_4$H$_9$)$_4$N(CF$_3$SO$_3$) (scan rate: 50 mV·s$^{-1}$); (b) Cyclic voltammogram for the solution of TlCF$_3$SO$_3$ in tmu/0.2 M ($n$-C$_4$H$_9$)$_4$N(CF$_3$SO$_3$).

not observed, Fig. 6b. Under the conditions of electrochemical measurements the oxidation of thallium(I) to thallium(III) was not achieved. As seen in Fig. 6a, the decrease of the peak at positive potential and increase of the peaks at negative values were registered in time. Moreover, a quite good linear correlation connected with the loss of thallium (III) amount with a half-life time of approximately 111.8 min is observed, Fig. S9, which is surprisingly about two times longer than that observed by the UV–Vis technique.

The determination of the half-life time of the studied system by UV–Vis spectroscopy may be burdened with considerable error due to a lack of a clear maximum absorbance point in the spectra. Therefore this value was estimated as an average value from a few different wavelengths. Similarly, in the case of electrochemical curves, some deviations in the position of the Tl(III)/Tl(I) reduction peak may have an impact on the correct $t_{1/2}$ value. In contrast to the solution of Tl(CF$_3$SO$_3$)$_3$ in tmu, no signal corresponding to the reduction of Tl(III) to Tl(I) was observed in the cyclic voltammetry curve for its solution in dmpu (Fig. S10).

## 4. Conclusions

When solid anhydrous thallium(III) trifluoromethanesulfonate, Tl (CF$_3$SO$_3$)$_3$, or thallium(III) trifluoroacetate, Tl(CF$_3$COO)$_3$, are dissolved in organic solvents as dimethylsulfoxide (dmso) and *N,N,N',N'*-tetramethylurea (tmu) a red-colored mixed-valence thallium(III)-thallium(I) complex is formed. This red thallium complex is stable in dmso for at least years, but it reduces fairly rapidly to thallium(I) in tmu with a half-life time of an hour, and in *N,N*-dimethylpropyleneurea (dmpu) an immediate reduction to thallium(I) takes place. In acidic aqueous solution, stable hydrated thallium(III) ions are obtained. The observations strongly indicate that the trifluoromethanesulfonate and trifluoroacetate ions play an essential role in the formation of the red thallium complex, even though they do not necessarily bind to thallium in the red complex formed. $^{205}$Tl NMR data show that the red thallium complex contains equal amounts of thallium(III) and thallium(I). The structure of the red thallium complex, as determined by EXAFS, shows Tl–O bond distances of 2.216(3) and 2.80(2) Å, which are in very close agreement with the bond distances obtained in the dmso solvates of the thallium(III) and thallium(I) ions, respectively [1,11], and a Tl···Tl distance of 3.49(1) Å bridged by oxygen atoms. It is not possible from the EXAFS data to distinguish if dmso molecules and/or trifluoromethanesulfonate ions act as bridges. DFT calculations indicate that dmso molecules bridge the thallium(I) and thallium(III) sites with a trifluoromethanesulfonate binding to the thallium(I) ion, which certainly reduces the repulsion between the two thallium sites. DFT calculations could also eliminate some structures due to the irrelevant structural parameters or the energetics of the proposed reactions based on the experimental studies. The striking stability of the red-colored

mixed-valence thallium complex in dmso, characterized in this study, makes it to an ideal strong oxidizing agent in kinetic redox studies due to the color change. Whether this mixed-valence thallium complex can be further stabilized by multi-dentate ligands is an area of future research, and possible use in e.g. nuclear medicine [34].

## CRediT authorship contribution statement

Conceptualization and project administration — Ingmar Persson. Data curation and formal analysis — NMR spectroscopy: Imre Tóth and Tibor Csupász, XAFS spectroscopy: Ingmar Persson and Kajsa Sigfridsson Clauss, UV-Vis spectrophotometry: Krzysztof Łyczko and Éva G. Bajnoczi, Cyclic voltammetry: Krzysztof Łyczko and Agnieszka Więckowska, DFT simulations: Mihály Purgel, Funding acquisition, investigation, resources, supervision and investigation — Imre Tóth, Krzysztof Łyczko and Ingmar Persson, Methodology, software and visualization — Ingmar Persson, Krzysztof Łyczko and Imre Tóth, Mihály Purgel Mihály Purgel, Writing original draft, review and editing — Ingmar Persson, Krzysztof Łyczko and Imre Tóth.

## Declaration of Competing Interest

The authors declare that they have no known competing financial interests or personal relationships that could have appeared to influence the work reported in this paper.

## Data availability

Data will be made available on request.

MAX IV, a Swedish national user facility, is supported by the Swedish Research council under contract 2018-07152, the Swedish Governmental Agency for Innovation Systems under contract 2018-04969, and Formas under contract 2019-02496.

## Appendix A. Supplementary material

Supplementary data to this article can be found online at https://doi.org/10.1016/j.molliq.2023.122233.

## References

[1] G. Ma, A. Molla-Abbassi, M. Kritikos, A. Ilyukhin, F. Jalilehvand, V. G.; Kessler, M. Skripkin, M. Sandström, J. Glaser, J. Näslund, I. Persson, I. Structure of the dimethyl sulfoxide solvated thallium(III) ion in solution and in the solid state. Inorg. Chem. 40 (2001) 6432–6438. 10.1021/ic010453k.

[2] M. Ghadermazi, F. Manteghi, Hexakis(dimethyl sulfoxide-*κO*) thallium(III) nitrate, Acta Crystallogr., Sect. E 66 (2010) m812–m, https://doi.org/10.1107/S1600536810022646.

[3] J. Glaser, G. Johansson, Crystal structures of the isomorphous perchlorate hexahydrates of of some trivalent metal ions (M=La, Tb, Er, Tl), Acta Chem. Scand., Ser A 35 (1981) 639–644, https://doi.org/10.3891/acta.chem.scand.35a-0639.

[4] J. Glaser, G. Johansson, On the structures of the hydrated thallium(III) ion and its bromide complexes in aqueous solution, Acta Chem. Scand., Ser A 36 (1982) 125–135, https://doi.org/10.3891/acta.chem.scand.36a-01025.

[5] J. Blixt, J. Glaser, J. Mink, I. Persson, P. Persson, M. Sandström, On the Structure of Thallium(III) Chloride, Bromide and Cyanide Complexes in Aqueous Solution, J. Am. Chem. Soc. 117 (1995) 5089–5104, https://doi.org/10.1021/ja00123a011.

[6] A. Molla-Abbassi, L. Eriksson, J. Mink, I. Persson, M. Sandström, M.Y. Skripkin, A.-S. Ullström, P. Lindqvist-Reis, Structure and bonding of bisaquamercury(II) and trisaquathallium(III) trifluoromethanesulfonate, J. Chem. Soc., Dalton Trans. (2002) 4357–4363, https://doi.org/10.1039/B206021N.

[7] M. Sandström, M. Crystal structure of hexaaquamercury(II) perchlorate, [Hg (H₂O)₆](ClO₄)₂. Acta Chem Scand., Ser. A 32 (1978) 32, 109–113. 10.3891/acta.chem.scand.32a-0109.

[8] F.H. Allen, The Cambridge Structural Database: a quarter of a million crystal structures and rising, Inorganic Crystal Structure Database 1.4.6 (release: 2022-2); FIZ/NIST. Acta Crystallogr., Sect. B 58 (2002) 380–388 https://10.1107/S0108768102002902;.

[9] J.M. Harrowfield, R.P. Sharma, B.W. Skelton, A.H. White, Structural Systematics of 2/4-nitrophenoxide complexes of closed shell metal ions. III 2/4-nitrophenoxides of univalent heavy metals, Aust. J. Chem. 51 (1998) 735–746, https://doi.org/10.1071/C97100.

[10] Y. Sarazin, D.L. Hughes, N. Kaltsoyannis, J.A. Wright, M. Bochman, Thallium(I) sandwich, multidecker, and ether complexes stabilized by weakly-coordinating anions: A spectroscopic, structural and theoretical investigation, J. Am. Chem. Soc. 129 (2007) 881–894, https://doi.org/10.1021/ja0657105.

[11] I. Persson, F. Jalilehvand, M. Sandström, Structure of the solvated thallium(I) ion in aqueous, dimethyl sulfoxide, *N, N*`-dimethylpopyleneurea and *N, N*-dimethylthioformamide solution, Inorg. Chem. 41 (2002) 192–197, https://doi.org/10.1021/ic010587y.

[12] J.F. Hinton, R.W. Briggs, Thallium-205 NMR spectroscopy. I. ²⁰⁵Tl⁺¹ chemical shifts a sensitive probe for preferential solvation and solution structure, J. Magn. Reson. 19 (1975) 393–397, https://doi.org/10.1016/0022-2364(75)90055-4.

[13] M. Sandström, I.; Persson, P. Persson, A study of solvent electron-pair donor ability and Lewis basicity scales. Acta Chem. Scand. 44 (1990) 653–675. 10.3891/acta.chem.scand.44-0653.

[14] N. V. Sidgwick, H. M. Powell, Bakerian lecture. Stereochemical types and valency groups. Proc. R. Soc. (London) 176 (1940) 153-180. 10.1098/rspa.1940.0084.

[15] R.J. Gillespie, R.S. Nyholm, Inorganic Stereochemistry. Q. Rev. London 11 (1957) 339–380, https://doi.org/10.1039/QR9571100339.

[16] R. J. Gillespie, I. Hargittai, I. The VSEPR Model of Molecular Geometry, Allyn and Bacon, Boston, MA, **1991**, ISBN-10: 020512-369-4.

[17] A.-V. Mudring, Stereochemical Activity of Lone Pairs in Heavier Main-group Element Compounds, in: G. Meyer, D. Naumann, L. Wesemann (Eds.), Inorganic Chemistry in Focus III, Wiley-VCH Verlag GmbH & Co. KGaA, Weinheim, Germany, 2006, pp 15–28.

[18] A.-V. Mudring, F. Rieger, Lone pair tffect in thallium(I) macrocyclic compounds, Inorg. Chem. 44 (2005) 6240–6243, https://doi.org/10.1002/ic050547k.

[19] A. Walsh, G.W. Watson, The origin of the stereochemically active Pb(II) lone pair: DFT calculations on PbO and PbS, J. Solid State Chem. 178 (2005) 1422–1428, https://doi.org/10.1016/j.jssc.2005.01.030.

[20] A.-V. Mudring, Thallium halides - New aspects of the stereochemical activity of electron lone pairs of heavier main-group elements. Eur. J. Inorg. Chem. (2007) 882–890, and references therein. 10.1002/ejic.200600975.

[21] L. Shimoni-Livny, J. P. Glusker, C. W. Bock, Lone pair functionality in divalent lead compounds. Inorg. Chem. 37 (1998) 1853–1867, and references therein. 10.1021/ic970909r.

[22] V. Ndoyom, L. Fusaro, V. Dorcet, B. Boitrel, S. Le Gac, Sunlight-Driven Formation and Dissociation of a Dynamic Mixed-Valence Thallium(III)/Thallium(I) Porphyrin

[23] Complex, Angew. Chem. 54 (2015) 3806–3811, https://doi.org/10.1002/anie.201411616.

[23] T. Firdoos, P. Kumar, A. Radha, R.M. Gomila, A. Frontera, P. Soodc, S.K. Pandey, An insight into triel bonds in O, O0-diarylphosphorodithioates of thallium(I): experimental and theoretical investigations, New J. Chem. 46 (2022) 832–843, https://doi.org/10.1039/d1nj04852j.

[24] K. Lyczko, M. Lyczko, M. Banasiewicz, K. Wegrzynska, A. Ziółko, A. Baraniak, J. C. Dobrowolski, Thallium(I) Tropolonates: Synthesis, Structure, Spectral Characteristics, and Antimicrobial Activity Compared to Lead(II) and Bismuth(III) Analogues, Molecules 27 (2022) 183, https://doi.org/10.3390/molecules27010183.

[25] M. Hammond, D.A. Vaccaro, G. Parkin, Synthesis and structural characterization of thallium and cadmium carbatrane compounds, [Tismᴾʳⁱᴮᵉⁿᶻ]Tl and [Tismᴾʳⁱᴮᵉⁿᶻ] CdMe, Polyhedron 222 (2022) 15642, https://doi.org/10.1016/j.poly.2021.115642.

[26] P. Vaňura, D. Sýkora, T. Uhlíková, Reaction of the thallium(I) cation with [2.2] paracyclophane: Experimental and theoretical study, Inorg. Chim. Acta 543 (2022), 121205, https://doi.org/10.1016/j.ica.2022.121205.

[27] G. Gomathi, E. Sathiyaraj, S. Thirumaran, S. Ciattini, Synthesis, spectral, structural and DFT studies on Tl(III) dithiocarbamate complexes: Preparation of Tl₂S nanoparticles from tris(N-benzyl-N-furfuryldithiocarbamato-S, S`)thallium(III), Results Chem. 5 (2023), 100780. https://doi.org/10.1016/j.rechem.2023.100780.

[28] H.J. Kim, A. Khan, J. Daniel, G. Rooh, P.Q. Vuong, Thallium-based heavy inorganic scintillators: recent developments and future perspectives, CrystEngComm 24 (2022) 450–464, https://doi.org/10.1039/d1ce01422f.

[29] M. Sohail, M. Husain, N. Rahman, K. Althubeiti, M. Algethami, A.A. Khan, A. Iqbal, A. Ullah, A. Khan, R. Khan, First-principal investigations of electronic, structural, elastic and optical properties of the fluoroperovskite TlLF₃ (L L̈ Ca, Cd) compounds for optoelectronic applications, RSC Adv. 12 (2022) 7002–7008, https://doi.org/10.1039/d2ra00464j.

[30] F. Caddeo, E. Fernández-Moreira, M. Arca, A. Pintus, A. Laguna, V. Lippolis, M. Concepción Gimeno, Luminescent gold–thallium derivatives with a pyridine-containing 12-membered aza-thioether macrocycle, Dalton Trans. 50 (2021) 9709–9718, https://doi.org/10.1039/d1dt01599k.

[31] R. Donamaría, V. Lippolis, J.M. López-de-Luzuriaga, M. Monge, M. Nieddu, M. E. Olmos, Structural and Luminescence Properties of Heteronuclear Gold(I)/thallium (I) Complexes Featuring Metallophilic Interactions Tuned by Quinoline Pendant Arm Derivatives of Mixed Donor Macrocycles, Inorg. Chem. 59 (2020) 6398–6409, https://doi.org/10.1021/acs.inorgchem.0c00469.

[32] C. Ma, H. Cheng, R. Huang, Y. Zou, Q. He, X. Huangfu, J. Ma, Kinetics of Thallium (I) Oxidation by Free Chlorine in Bromide-Containing Waters: Insights into the Reactivity with Bromine Species, Environ. Sci. Technol. 56 (2022) 1017–1027, https://doi.org/10.1021/acs.est.1c06901.

[33] C. Ma, R. Huang, X. Huangfu, J. Ma, Q. He, Light- and H₂O₂–Mediated Redox Transformation of Thallium in Acidic Solutions Containing Iron: Kinetics and Mechanistic Insights, Environ. Sci. Technol. 56 (2022) 5530–5541, https://doi.org/10.1021/acs.est.2c00034.

[34] A. Rigby, G. Firth, C. Rivas, T. Pham, J. Kim, A. Phanopoulos, L. Wharton, A. Ingham, L. Li, M.T. Ma, C. Orvig, P.J. Blower, S.Y.A. Terry, V. Abbate, Toward Bifunctional Chelators for Thallium-201 for Use in Nuclear Medicine, Bioconjugate Chem. 33 (2022) 1422–1436, https://doi.org/10.1021/acs.bioconjchem.2c00284.

[35] S. Abdolmaleki, M. Ghadermazi, A. Aliabadi, Novel Tl(III) complexes containing pyridine–2,6-dicarboxylate derivatives with selective anticancer activity through inducing mitochondria–mediated apoptosis in A375 cells, Sci. Rep. 11 (2021) 15699, https://doi.org/10.1038/s41598-021-95278-y.

[36] TopSpin© software (ver. 3.6.2), Bruker BioSpin GmbH, Bruker Corp., Rheinstetten, Germany. (https://www.bruker.com/en/products-and-solutions/mr/nmr-software/topspin.html).

[37] K. Klementiev, K. Norén, S. Carlson, K.G.V. Sigfridsson Clauss, I. Persson, The Balder beam-line at the MAX IV laboratory, J. Phys.; Conf. Ser. 712 (2016), 012023, https://doi.org/10.1088/1742-6596/712/012023.

[38] I. Persson, D. Lundberg, É.G. Bajnoczi, K. Klementiev, J. Just, K.G.V. Sigfridsson Clauss, An EXAFS study on the coordination chemistry of the solvated copper(II) ion in a series of solvents using data collected at the new XAS beam-line Balder at the MAX IV synchrotron light facility, Inorg. Chem. 59 (2020) 9538–9550, https://doi.org/10.1021/acs.inorgchem.0c00403.

[39] A. Thompson, D. Attwood, E. Gullikson, M. Howells, K.-J. Kim, J. Kirz, I. Lindau, Y. Liu, P. Pianetta, A. Robinson, J. Scofield, J. Underwood, D. Vaughan, G. Williams, H. Winick, H. X-ray data booklet, Lawrence Berkeley National Laboratory, Berkeley, 3ʳᵈ rev., 2009.

[40] G. N. George, I. J. Pickering, EXAFSPAK - A suite of computer programs for analysis of X-ray absorption spectra, 2000; available at: https://www-ssrl.slac.stanford.edu/exafspak.html.

[41] S.I. Zabinsky, J.J. Rehr, A. Ankudinov, Multiple Scattering Calculations of X-ray Absorption Spectra, Phys. Rev. B. 52 (1995) 2995–3009, https://doi.org/10.1103/PhysRevB.52.2995.

[42] M. J. Frisch, G. W. Trucks, H. B. Schlegel, G. E. Scuseria, M. A. Robb, J. R. Cheeseman et al. 2010, Gaussian 09. Revision C.01. Wallingford: Gaussian Inc.

[43] Y. Zhao, D.G. Truhlar, The M06 suite of density functionals for main group thermochemistry, thermochemical kinetics, noncovalent interactions, excited states, and transition elements: two new functionals and systematic testing of four M06-class functionals and 12 other functionals, Theor. Chem. Acc. 120 (2008) 215–241, https://doi.org/10.1007/s00214-007-0310-x.

[44] A. Schäfer, C. Huber, R. Ahlrichs, Fully optimized contracted Gaussian-basis sets of triple zeta valence quality for atoms Li to Kr, J. Chem. Phys. 100 (1994) 5829–5835, https://doi.org/10.1063/1.467146.

[45] R.B. Ross, J.M. Powers, T. Atashroo, W.C. Ermler, L.A. LaJohn, P.A. Christiansen, Ab initio relativistic effective potentials with spin-orbit operators. IV. Cs through Rn, J. Chem. Phys. 93 (1990) 6654–6670, https://doi.org/10.1063/1.458934.

[46] S. Miertuš, E. Scrocco, J. Tomasi, Electrostatic interaction of a solute with a continuum. A direct utilization of ab initio molecular potentials for the prevision of solvent effects, Chem. Phys. 55 (1981) 117–129, https://doi.org/10.1016/0301-0104(81)85090-2.

[47] W.A. Ayass, T. Fodor, E. Farkas, Z. Lin, H.M. Qasim, S. Bhattacharya, A. S. Mougharbel, K. Abdallah, M.S. Ullrich, S. Zaib, J. Iqbal, S. Harangi, G. Szalontai, I. Bányai, L. Zékány, I. Tóth, U. Kortz, Dithallium(III)-containing 30-tungsto-4-

phosphate, $[Tl_2Na_2(H_2O)_2(P_2W_{15}O_{56})_2]^{16-}$: Synthesis, structural characterization, and biological studies, Inorg. Chem. 57 (2018) 7168–7179, https://doi.org/10.1021/acs.inorgchem.8b00878.

[48] W.W. Ayass, T. Fodor, Z. Lin, R.M. Smith, X. Xing, K. Abdallah, I. Tóth, L. Zékány, M. Pascual-Borràs, A. Rodríguez-Fortea, J.M. Poblet, L. Fan, J. Cao, B. Keita, M. S. Ullrich, U. Kortz, Inorg. Chem. 55 (2016) 10118–10121, https://doi.org/10.1021/acs.inorgchem.6b01921.

[49] A. Bodor, I. Banyai, J. Kowalewski, J. Glaser, Thallium(III) coordination compounds: chemical information from [205]Tl NMR longitudinal relaxation times, Magn. Reson. Chem. 40 (2002) 716–722, https://doi.org/10.1002/mrc.1077.